MITSUBISHI ELECTRIC RESEARCH LABORATORIES
http://www.merl.com

Multi-Dimensional Pulse-Shaping FIR Filter for Nonlinear Interference Alignment

Koike-Akino, T.; Millar, D.S.; Parsons, K.; Kojima, K.

TR2018-016 March 2018

Abstract

We design an irregular pulse-shaping filter to mitigate nonlinear distortion in optical fiber transmission. Our optimized four-dimensional filter allowing nonphysical rotations achieves up to 0.55 dB gain over standard root-raised-cosine (RRC) Nyquist shaping.

Optical Fiber Communication Conference and Exposition and the National Fiber Optic Engineers Conference (OFC/NFOEC)

Multi-Dimensional Pulse-Shaping FIR Filter for Nonlinear Interference Alignment

Toshiaki Koike-Akino, David S. Millar, Kieran Parsons, Keisuke Kojima

Mitsubishi Electric Research Laboratories (MERL), Cambridge, MA 02139, USA. *koike@merl.com*

Abstract: We design an irregular pulse-shaping filter to mitigate nonlinear distortion in optical fiber transmission. Our optimized four-dimensional filter allowing nonphysical rotations achieves up to 0.55 dB gain over standard root-raised-cosine (RRC) Nyquist shaping.

OCIS codes: (060.4510) Optical communications, (060.1660) Coherent communications, (060.4080) Modulation.

1. Introduction

The effect of pulse shaping in optical communications has been investigated in literature [1–10]. For example, it was shown experimentally that a return-to-zero (RZ) pulse increases maximum reach by 18% and 13% for dual-polarization 4-ary quadrature-amplitude modulation (DP-4QAM) [2] and DP-16QAM [3], respectively. The performance gain is explained by the fact that a wider spectrum can reduce the nonlinear interference (NLI) due to the decreased coherence between neighboring frequency components along the fiber propagation. According to such a spectrum broadening concept, an impulsive shape with Nyquist condition was numerically optimized by sequential quadratic programming (SQP) [4,5]. To further improve the performance in wavelength division multiplexing (WDM), staircase pulse [6] and root M-shaped pulse (RMP) [7–10], were later proposed. It was experimentally verified [10] that the RMP offers better performance than the impulsive shape [4,5] and the maximum reach can be increased by more than 11.7% at an excess bandwidth ratio (i.e., rolloff factor) of $\alpha = 0.5$ in comparison to classical root-raised-cosine (RRC) filtering.

In this paper, we adopt alternating minimization techniques used for interference alignment (IA) [11] to design a finite-impulse response (FIR) filter so that the non-white NLI is minimized. We show that the optimized FIR filter can outperform RRC and RMP filters, by at least 0.3 dBQ, in DP-16QAM transmission with dispersion unmanaged fiber links. In addition, we show that an optimized four-dimensional (4D) FIR filter, which exploits additional degree of freedom (DoF) allowing nonphysical state-of-polarization (SOP) rotations [12], achieves additional gain of 0.1 dB.

2. FIR Filter Optimization with Alternating Minimization Interference Alignment

A schematic of the simulated system is depicted in Fig. 1. Nine DP-16QAM channels at a baud rate of 34 GBd with 50 GHz spacing are multiplexed at a transmitter (Tx), and propagated over multiple 80 km spans of standard single mode fiber (SSMF) without inline dispersion compensation, using split-step Fourier method with an adaptive step-size Manakov model. We assume an attenuation of 0.2 dB/km, dispersion factor of $D = 17$ ps/nm/km, and nonlinearity factor of $\gamma = 1.2$ /W/km for SSMF. The fiber loss is compensated using an ideal Erbium-doped fiber amplifier (EDFA) every span. All amplified spontaneous emission (ASE) noise (noise figure of 5 dB) are applied just before the receiver (Rx). Both the Tx and Rx employ 50% chromatic dispersion compensation via frequency domain processing. An adaptive linear equalizer (LEQ) is used to compensate for any residual intersymbol interference. The Rx FIR taps for the LEQ are determined with data-directed minimum mean-square error (MMSE). We use a four-dimensional $(2L+1)$-tap Rx equalization with two-times oversampling for a half-tap length of $L = 31$. Let $\boldsymbol{G}_l \in \mathbb{R}^{4\times 4}$ be the l-th tap ($l \in \{-L,\ldots,L\}$, $\mathbb{R}$ being real numbers) to convolute with four-dimensional received DP-QAM signals.

NLI is usually non-white unlike ASE noise, and it is highly dependent on Tx power spectrum density (PSD) as shown in Fig. 2, where NLI spectrum is computed by the Gaussian noise (GN) model [13] for RRC and RMP filters (with a rolloff factor of $\alpha = 0.40$ and a depth factor of $\beta = 0$). The NLI non-whiteness can be exploited to optimize pulse-shaping filter so that NLI can be suppressed at a certain band where higher signal power is allocated. For example, RMP filter allocates high signal power at the ends of band (e.g., $|f| \simeq 24$GHz), in which NLI is usually weaker, resulting into approximately 2 dB lower NLI compared to RRC in the sideband regimes as shown in Fig. 2.

We consider a $(2L+1)$-tap symmetry FIR Tx filter such that $\boldsymbol{F}_l = \boldsymbol{F}_{-l}$, where $\boldsymbol{F}_l \in \mathbb{R}^{4\times 4}$ denotes the l-th tap coefficient. Conventional pulse uses an identical FIR filter for 4D DP-QAM signals, using scalar FIR taps $F_l \in \mathbb{R}$ as $\boldsymbol{F}_l = F_l \cdot \boldsymbol{I}$ ($\boldsymbol{I}$ is an identity matrix). We call it 1D FIR pulse shaping (having 1DoF per tap). We show that the

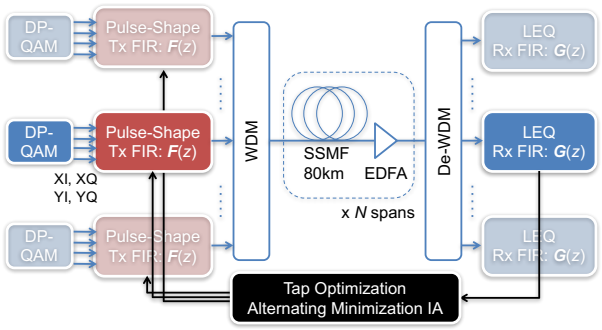

Fig. 1: Nonlinear fiber transmission systems with offline optimization of pulse-shaping FIR filter $\boldsymbol{F}(z)$ via alternating minimization interference alignment given Rx FIR filter $\boldsymbol{G}(z)$, simulated with test sequence in advance.

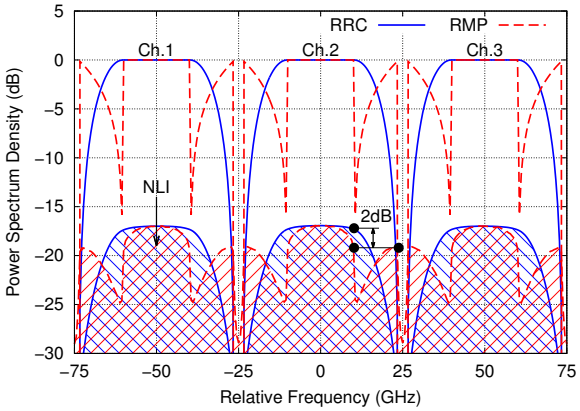

Fig. 2: NLI spectrum predicted by GN model [13] for RRC and RMP pulse shaping [7–10] ($\alpha = 0.4$, $\beta = 0.0$).

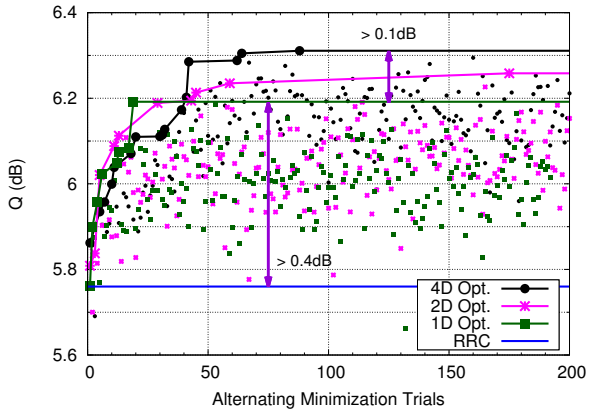

Fig. 3: FIR optimization trajectory via alternating minimization IA [11] (60 spans, 0 dBm, $\alpha = 0.47$).

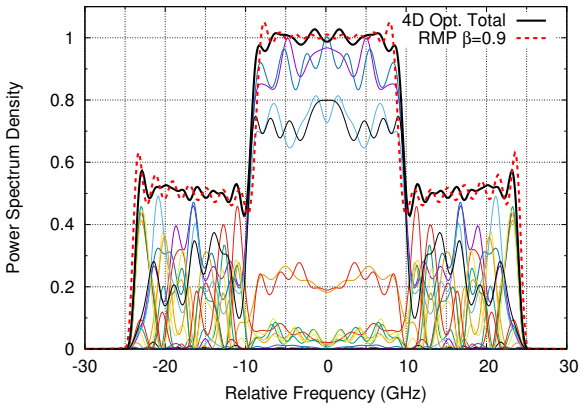

Fig. 4: Optimized 4D FIR filter (60 spans, 0 dBm, $\alpha = 0.47$): 16 curves for $\boldsymbol{F}$ and total transfer function $\|\boldsymbol{F}\|$.

proposed 4D FIR pulse shaping (having $4 \times 4 = 16$DoF) is advantageous in NLI suppression. Note that the 4D FIR filter enables nonphysical SOP rotations [12]. For a singular value decomposition $\boldsymbol{F}_l = \boldsymbol{U}_l \boldsymbol{\Lambda}_l \boldsymbol{V}_l$, both the left and right singular matrices ($\boldsymbol{U}_l$ and $\boldsymbol{V}_l$) have 6DoF, four of which correspond to linear/circular birefringence and phase rotations according to [12]. Since the remaining DOF are physically infeasible in optics, we can consider a lower-DoF FIR filter design removing nonphysical 4DoF. For this case, FIR taps can be equivalently expressed by complex-valued matrices $\boldsymbol{F}_l \in \mathbb{C}^{2\times 2}$ (having 8DoF, $\mathbb{C}$ being complex numbers). We refer to it as 2D FIR pulse shaping for convenience.

In order to optimize pulse-shaping FIR filters $\boldsymbol{F}_l$ with/without DoF constraints, we introduce the alternating minimization approach used for IA [11]. This method relies on the principle that non-white correlated interference can be minimized by iterating a successive MMSE process which simply replaces the Tx filter with the Rx MMSE filter. Fig. 3 shows the optimization trajectory across the alternating minimization IA, where the RRC filter taps are used as the initial values, for 60 spans at a per-channel launch power of 0 dBm. For each optimization trial, the Tx FIR tap coefficients $\boldsymbol{F}_l$ are replaced with the Rx FIR tap coefficients $\boldsymbol{G}_l$, using a randomly generated DP-16QAM test sequence of 2^{14} symbols each iteration. It is observed from Fig. 3 that a few tens of iterations offer more than 0.4 dB improvement. In addition, we observe that the 4D FIR pulse shaping with no constraint in DoF for $\boldsymbol{F}_l \in \mathbb{R}^{4\times 4}$ outperforms 1D FIR Tx filter by greater than 0.1 dB, and more importantly, it is still 0.05 dB better than 2D FIR filter.

Fig. 4 show the transfer function of the optimized 4D FIR filter. Interestingly, the total transfer function $\|\boldsymbol{F}\|$ of optimized 4×4 FIR filter $\boldsymbol{F}_l$ looks like RMP with $\beta \simeq 0.9$ (ripple is due to finite tap truncation) even though RRC was used as the initial FIR tap for alternating minimization. Nevertheless, our optimized 4D filter exhibits more complicated SOP rotations across frequency in particular at sideband regimes. This frequency-varying SOP scrambling may improve the nonlinear performance. More importantly, the optimized FIR filter contains nonphysical rotations; e.g., at $f = 20$ GHz, $\boldsymbol{V} = \exp(-0.79\boldsymbol{\rho}_1 + 0.26\boldsymbol{\rho}_2 + 0.84\boldsymbol{\rho}_3 - 0.70\boldsymbol{\lambda}_1 + 0.29\boldsymbol{\lambda}_2 - 0.90\boldsymbol{\lambda}_3)$, where $\boldsymbol{\rho}_i$ and $\boldsymbol{\lambda}_i$ are 4D rotation bases [12]. The nonzero coefficients for $\boldsymbol{\lambda}_2$ and $\boldsymbol{\lambda}_3$ indicate contributions from nonphysical SOP rotations.

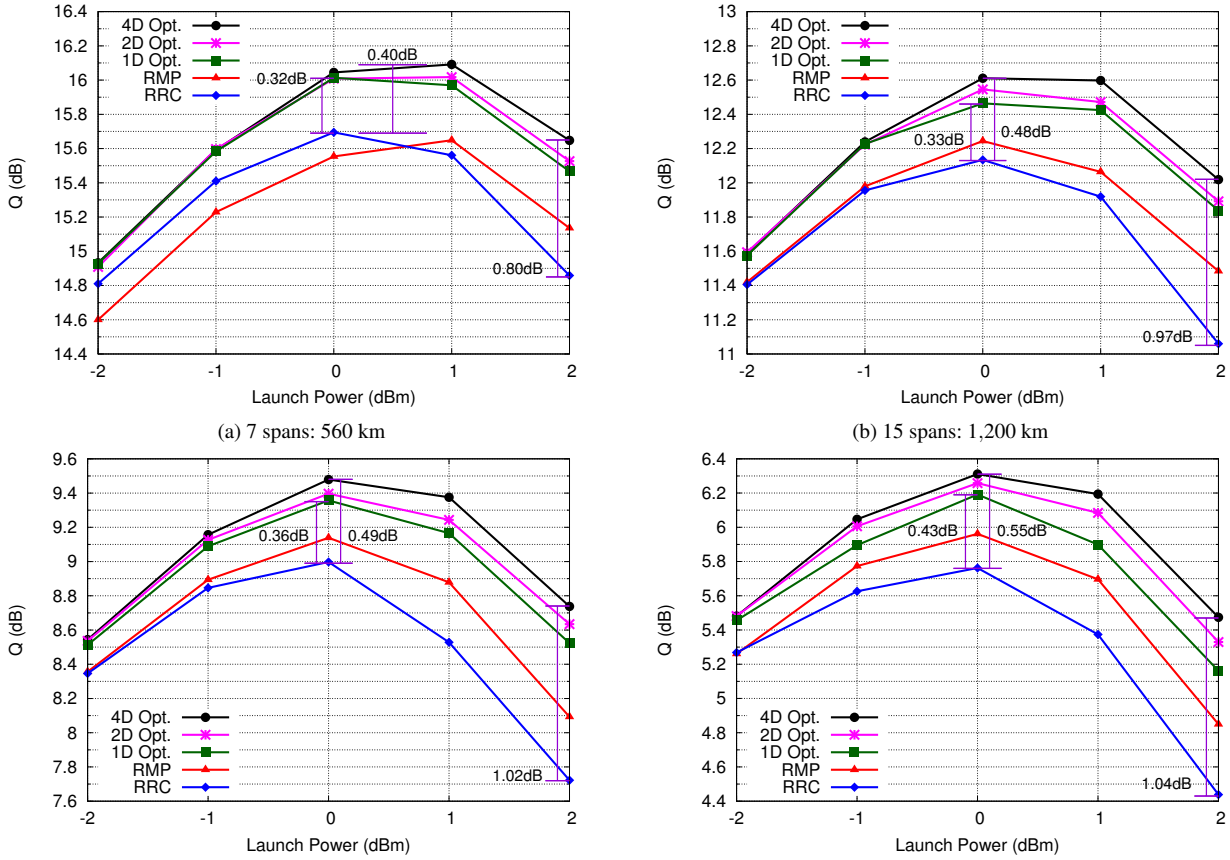

(a) 7 spans: 560 km

(b) 15 spans: 1,200 km

(c) 30 spans: 2,400 km

(d) 60 spans: 4,800 km

Fig. 5: Nonlinear transmission performance of DP-16QAM in dispersion-unmanaged SSMF links.

3. Nonlinear Transmission Performance and Summary

Fig. 5 shows the simulated nonlinear transmission performance for 7, 15, 30, and 60 spans of dispersion unmanaged SSMF links. We can see that our optimized 1D FIR pulse shaping achieves 0.32–0.43 dB improvement at peak Q factor in comparison to the conventional RRC pulse shaping. Note that the RMP filter ($\beta = 0.9$) does not perform better than our designed FIR filters, especially for shorter fiber distances. It is also verified that the optimized 4D FIR pulse shaping can further improve the nonlinearity tolerance. For 60 spans, a remarkable gain of 0.55 dB was achieved by the 4D filter, and a more significant gain can be obtained in the highly nonlinear regimes. The advantage of nonphysical SOP rotations was found to be greater than 0.05 dB comparing to the optimized 2D pulse shaping.

We designed a pulse-shaping FIR filter via alternating minimization IA to suppress NLI, achieving greater than 0.3 dBQ compared to the conventional RRC filter. In addition, we showed that an additional 0.1 dB gain can be obtained by optimizing 4D FIR filters which exploit nonphysical SOP rotations.

References

1. E. Torrengo et al., "Influence of pulse shape in 112-Gbit/s WDM PDM-QPSK transmission," *IEEE PTL* **22** 23 (2010): 1714–1716.
2. S. Makovejs et al., "Comparison of pulse shapes in a 224 Gbit/s (28 Gbaud) PDM-QAM16 long-haul transmission experiment," *OFC* (2011): OMR5.
3. C. Behrens et al., "Pulse-shaping versus digital backpropagation in 224Gbit/s PDM-16QAM transmission," *Opt. Expr.* **19** 14 (2011).
4. B. Châtelain et al., "SPM-tolerant pulse shaping for 40- and 100-Gb/s dual-polarization QPSK systems," *IEEE PTL* **22** 22 (2010): 1641–1643.
5. B. Châtelain et al., "Optimized pulse shaping for intra-channel nonlinearities mitigation in a 10 Gbaud dual-polarization 16-QAM system," *OFC* (2011): OWO5.
6. B. Châtelain et al., "A family of Nyquist pulses for coherent optical communications," *Opt. Expr.* **20** 8 (2012): 8397–8416.
7. X. Xu et al., "Frequency domain M-shaped pulse for SPM nonlinearity mitigation in coherent optical communications," *OFC* (2013): JTh2A-38.
8. X. Xu et al., "Nonlinearity-tolerant frequency domain root M-shaped pulse for spectrally efficient coherent transmissions," *Opt. Expr.* **21** 26 (2013).
9. X. Xu et al., "Nonlinearity-tolerant frequency domain root M-shaped pulse for spectrally efficient coherent transmissions," *OFC* (2014): W1G-3.
10. —, "Experimental investigation on the nonlinear tolerance of root M-shaped pulse in spectrally efficient coherent transmissions," *Opt. Expr.* **23** 2 (2015).
11. K. Gomadam et al., "Approaching the capacity of wireless networks through distributed interference alignment," *GLOBECOM* (2008).
12. M. Karlsson, "Four-dimensional rotations in coherent optical communications," *JLT* **32** 6 (2014): 1246–1257.
13. P. Poggiolini, "The GN model of non-linear propagation in uncompensated coherent optical systems," *JLT* **30** 24 (2012): 3857–3879.